haematologica
Journal of The Ferrata Storti Foundation

Single-cell profiling reveals the dynamics of cytomegalovirus-specific T-cells in haploidentical hematopoietic stem cell transplantation

by Jasper J. P. van Beek, Simone Puccio, Alessandra Roberto, Federica De Paoli, Giulia Graziano, Elisa Salviato, Giorgia Alvisi, Veronica Zanon, Alice Scarpa, Elisa Zaghi, Michela Calvi, Clara Di Vito, Rossana Mineri, Barbara Sarina, Chiara De Philippis, Armando Santoro, Jacopo Mariotti, Stefania Bramanti, Francesco Ferrari, Luca Castagna, Domenico Mavilio, and Enrico Lugli

Haematologica 2021 [Epub ahead of print]

Citation: Jasper J. P. van Beek, Simone Puccio, Alessandra Roberto, Federica De Paoli, Giulia Graziano, Elisa Salviato, Giorgia Alvisi, Veronica Zanon, Alice Scarpa, Elisa Zaghi, Michela Calvi, Clara Di Vito, Rossana Mineri, Barbara Sarina, Chiara De Philippis, Armando Santoro, Jacopo Mariotti, Stefania Bramanti, Francesco Ferrari, Luca Castagna, Domenico Mavilio, and Enrico Lugli. Single-cell profiling reveals the dynamics of cytomegalovirus-specific T-cells in haploidentical hematopoietic stem cell transplantation. Haematologica. 2021; 106:xxx doi:10.3324/haematol.2020.276352

Single-cell profiling reveals the dynamics of cytomegalovirus-specific T-cells in haploidentical hematopoietic stem cell transplantation

Jasper J. P. van Beek[1,*], Simone Puccio[1], Alessandra Roberto[1,*], Federica De Paoli[1], Giulia Graziano[2], Elisa Salviato[2], Giorgia Alvisi[1], Veronica Zanon[1], Alice Scarpa[1], Elisa Zaghi[1], Michela Calvi[1], Clara Di Vito[3], Rossana Mineri[1], Barbara Sarina[1], Chiara De Philippis[1], Armando Santoro[1,4], Jacopo Mariotti[1], Stefania Bramanti[1], Francesco Ferrari[2,5], Luca Castagna[1], Domenico Mavilio[1,3], and Enrico Lugli[1]

[1] IRCCS Humanitas Research Hospital, Rozzano, Milan, Italy
[2] IFOM, the FIRC Institute of Molecular Oncology, Milan, Italy
[3] Department of Medical Biotechnologies and Translational Medicine (BioMeTra), University of Milan, Milan, Italy
[4] Department of Biomedical Sciences, Humanitas University, Pieve Emanuele, Milan, Italy
[5] IGM-CNR, Institute of Molecular Genetics "Luigi Luca Cavalli Sforza", National Research Council, Pavia, Italy

*These authors contributed equally to this work

Disclosures

This work was funded by the European Research Council (ERC_StG_2014 PERSYST #640511 to E.L.). The purchase of a FACSymphony A5 was defrayed in part by a grant from the Italian Ministry of Health (agreement 82/2015). E.L. receives reagents in kind from BD Biosciences Italy as part of a collaborative research agreement, and preclinical funding from Bristol-Myers Squibb on topics unrelated to the content of this manuscript. A.S. has received honoraria as advisory board member from Bristol-Myers Squibb, Servier, Gilead, Pfizer, Eisai, Bayer and Merck Sharp & Dhome; as speaker's bureau member from Takeda, Roche, Abb-vie, Amgen, Celgene, Astrazeneca, Lilly, Sandoz, Novartis, Bristol-Myers Squibb, Servier, Gilead, Pfizer, Arqule, Eisai; and for consultancy from Arqule. The other authors declare no financial interests.

Contributions:

J.J.P.v.B., A.R. and E.L. conceived the study; F.D.P., G.A., V.Z., A.S., E.Z., M.C. and C.D.V. performed the experiments; R.M., B.S., C.D.P., A.S., J.M., S.B. and L.C. collected the patient specimens and clinical data; J.J.P.v.B., S.P., A.R., G.G. and E.S. analyzed the data; J.J.P.v.B. and E.L. wrote the manuscript; F.F., L.C., D.M. and E.L. supervised the study. All authors contributed to and approved the final manuscript.

HLA-haploidentical hematopoietic stem cell transplantation (haplo-HSCT) with post-transplant cyclophosphamide (pt-cy) is a valid alternative to HLA-identical HSCT,[1] but many patients still suffer from viral infections, mostly cytomegalovirus (CMV) reactivation.[2] CMV-specific T-cells contribute to control of CMV reactivation post-transplant, but their evaluation has been limited to a handful of immunophenotypic parameters. In particular, the dynamics and quality of CMV-specific T-cells in relation to immune reconstitution and control of CMV viremia following haplo-HSCT with pt-cy are poorly known. To these aims, we employed high-dimensional flow cytometry simultaneously investigating 4 effector functions and markers of T-cell differentiation, inhibitory molecules, and metabolic and activation markers, along with computational analysis of single-cell data.

We performed longitudinal analysis of high-dimensional T-cell immunophenotypes in blood samples of 21 recipients of haplo-HSCT with pt-cy treated at our institution for hematological diseases (Supplementary Table S1). A median of 7 samples per patient were analyzed, including graft (n=13) and peripheral blood (PB) samples ranging from day +21 to day +386 post-transplant (n=111). As control, we included PB samples from donors (n=9) and healthy individuals with detectable CMV pp65-specific T-cells (n=17). The clustering tool PhenoGraph[3] identified 13 $CD8^+$ and 11 $CD4^+$ T-cell clusters (Figure 1A). Principle component analysis (PCA) of cluster frequencies identified which of the 24 T-cell clusters were co-varying in a time-dependent manner. A variable plot of the first two principle components revealed 4 major groups of T-cell phenotypes (Figure 1B). Median PCA coordinates of all samples plotted at defined intervals indicated a clear pattern in T-cell dynamics: loss of naïve and $CD73^+$ memory clusters and emergence of proliferating clusters at 3-4 weeks post-transplant, dominance of non-proliferating, activated clusters at month 2

and accumulation of effector and terminal effector (T_{TE}) clusters from month 3 onwards (Figure 1B).

Pt-cy interferes with highly-proliferating alloreactive T-cells, and alloreactivity resides preferentially in the naïve pool.[4–6] Furthermore, naïve cells that escape pt-cy may initially acquire a stem cell memory phenotype to later give rise to effector cells.[6,7] These processes may explain the rapid decline in naïve T-cells early after transplant. By week 3-4, Ki-67^{+}HLA-DR^{+} proliferating CD8^{+} cluster 10 and CD4^{+} cluster 9 expanded (Figure 1A), likely in response to a combination of exogenous or alloreactive antigens, homeostatic cytokines and inflammation.[6,7] The frequency of proliferating cells declined by month 2 and was accompanied by an increase in activated CD8^{+} and CD4^{+} Ki-67^{-}HLA-DR^{+} T-cells (cluster 6 and 4, respectively) that persisted for several months. CD4^{+} cluster 8 of regulatory T-cells (T_{REG}) and CD8^{+} cluster 13 of TIM-3^{high}PD-1^{high}TIGIT^{high} cells resembling exhausted cells, displayed dynamics similar to that of proliferating cells (Figure 1A). Transient T_{REG} expansion following haplo-HSCT with pt-cy corroborates previous findings[6,8] and seems critical for the prevention of graft-versus-host disease (GVHD) by pt-cy.[8,9] From month 3 onwards, the T-cell compartment became dominated by T_{TE} or effector memory re-expressing CD45RA (T_{EMRA}) clusters, expressing T-bet, 2B4, CD45RA and/or senescence marker CD57. One year after transplant, cluster distribution within the CD4^{+} compartment resembled that of the donor, including partial recovery of the naïve pool, while that within the CD8^{+} compartment showed a persistent defect in this regard (Figure 1A).

CMV infection is a major event following haplo-HSCT with pt-cy.[2] In our cohort, 19 out of 21 patients experienced CMV viremia, with a median onset of 39 days post-transplant. To

determine the effect of CMV viral load on T-cell reconstitution, we divided patients experiencing post-transplant CMV viremia into two groups using a viremia threshold above which antiviral therapy was given: subclinical CMV viremia (any viremia with peak ≤ 4000 IU/mL; *n*=6) and clinical CMV viremia (peak viremia > 4000 IU/mL; *n*=13). PCA of T-cell immunophenotypes indicated an accelerated acquisition of T-bet^{+}2B4^{+}CD45RA$^{+/-}$CD57$^{+/-}$ effector/terminal effector cells in patients with clinical CMV viremia (Group IV of CD8 clusters 2, 4, 5, 9 and CD4 clusters 6, 10; Figure 1B). These cells originated from both the CD8^{+} and CD4^{+} compartment, reaching statistically significant differences for T_{EMRA} cells in the former (Figure 1C and D). Furthermore, patients with subclinical viremia showed slightly improved recovery of naïve CD8^{+} T-cells. Although limited to 2 individuals in our cohort, those patients who did not experience CMV viremia lacked T_{TE} clusters and instead showed strong recovery of naïve subsets (Figure 1B). Accordingly, Suessmuth *et al.* found a decrease in naïve CD8^{+} T-cells in CMV-reactivating patients receiving unmanipulated unrelated allografts, suggesting a link between CMV reactivation and a defect in thymopoiesis.[10] Occurrence of clinically significant grade II-IV acute GVHD (aGVHD) and/or its treatment with corticosteroids could be a confounding factor and indeed tended to associate with worse CMV control in our cohort (Supplementary Figure S1A). However, hierarchical clustering indicated that patients developing aGVHD or receiving corticosteroids displayed overlapping T-cell cluster dynamics with aGVHD-negative patients (Figure 1E). These data suggest that CMV reactivation has a more prominent effect on T-cell reconstitution than does aGVHD, which is in line with findings at the clonal level in the HLA-matched setting.[11] Collectively, our data suggest that high CMV viral load drives premature senescence of T-cells and delays recovery of naïve T-cells following haplo-HSCT with pt-cy.

We next analyzed the functional and phenotypic profile of CMV-specific T-cells, identified through effector cytokines produced in response to CMV pp65 peptide library stimulation. Although likely underestimating the full extent of the CMV-directed T-cell response, which involves a broad range of antigens, pp65-specific T-cell responses are largely representative of the total response against CMV.[12] Uniform Manifold Approximation and Projection (UMAP) revealed dynamic changes in CMV-specific T-cell phenotypes during reconstitution (Figure 2A). PhenoGraph analysis of CMV-specific T-cells generated 15 $CD8^+$ and 14 $CD4^+$ T-cell clusters (Figure 2B). At week 3-4 post-haplo-HSCT, CMV-specific T-cells were undetectable in most patients. By month 2, in which CMV viremia emerged in the majority of patients, both $CD8^+$ and $CD4^+$ CMV-specific T-cells expanded and displayed a proliferating phenotype, featuring high levels of Ki-67, HLA-DR, CD71, PD-1, CD95 and CD98 (Figure 2B and Supplementary Figures S1B and S2A). From month 3, these phenotypes were replaced by effector phenotypes expressing T-bet, often in conjunction with CD57 and/or CD45RA, indicative of terminal differentiation. Although $CD8^+$ and $CD4^+$ CMV-specific T-cell immunophenotypes displayed similar dynamics, we also observed lineage-specific differences, including identification of multifunctional $CD4^+$ cluster 4 that highly expressed IL-2, IFN-γ, TNF and intermediate levels of CD107a. CMV-specific $CD8^+$ T-cells rarely expressed IL-2, rather, they commonly expressed IFN-γ and TNF. IFN-γ^-TNF$^+$ $CD8^+$ T-cells formed a minority, whereas IFN-γ^+TNF$^+$ T-cells were commonly seen and dominated the overall response from month 5. Interestingly, we identified $CD4^+$ clusters 3 and 11 expressing high levels of CD107a, T-bet, IFN-γ, TNF and CD57, reminiscent of killer-like cells otherwise identified in the $CD8^+$ compartment. Overall, the CMV-specific T-cell response showed maturation of effector functions over time (acquisition of at least 3 functions simultaneously), most prominently among $CD8^+$ T-cells (Figure 2C). The frequency of both

$CD8^+$ and $CD4^+$ CMV-specific T-cells in the PB of haplo-HSCT patients was greatly increased compared to that of the graft and PB of CMV-seropositive donors or PB of unrelated healthy controls, but phenotype distribution at 1 year was remarkably similar, suggesting reestablishment of physiological homeostasis (Figure 2D).

We next asked whether control of CMV viremia is associated with a greater abundance, or a specific functional or phenotypic profile, of CMV-specific T-cells. Huntley *et al.* reported >1 and >1.2 counts/μL of IFN-γ^+ CMV-specific $CD8^+$ and $CD4^+$ T-cells, respectively, to protect against reactivation following haplo-HSCT with pt-cy,[13] but other studies, predominantly on HLA-matched HSCT recipients, reported that multifunctional responses have a stronger predictive value.[14,15] We did not detect a significant difference in the total count of CMV-specific $CD8^+$ or $CD4^+$ T-cells in the first half-year post-transplant between patients with subclinical versus clinical CMV viremia, although CMV-specific $CD4^+$ T-cells tended to be present in higher amounts among patients with subclinical CMV (Figure 3A). Significant differences may occur at later time points, but our analysis was limited by the low number of patient samples at these time points. Analyzing the dynamics of each T-cell cluster separately, we found lower counts of multifunctional (cluster 4), proliferating (sum of phenotypically similar clusters 8 and 10) and T_{TE} T_H1 (sum of phenotypically similar clusters 2 and 9) $CD4^+$ T-cells at month 3-4 for patients with clinical viremia (Figure 3B). Although the size of each given patient group is low, patients with repeated CMV episodes requiring multiple treatment cycles tended to develop even lower counts of these T-cell phenotypes (Supplementary Figure S2B). No such trends were seen in the $CD8^+$ T-cell compartment (data not shown), thereby suggesting that control of CMV viremia post-haplo-HSCT mainly

associates with the development of distinct antigen-specific $CD4^+$ T-cell immunophenotypes.

In conclusion, CMV-specific T-cells were primed early after haplo-HSCT with pt-cy and initially displayed a proliferating/activated phenotype, that was quickly replaced by a terminal effector phenotype. One year after transplant, CMV-specific T-cell profiles were similar to those of the CMV-seropositive donor, suggesting reestablishment of physiological homeostasis. Uncontrolled viral replication associated with lower abundance of distinct CMV-specific $CD4^+$ T-cell immunophenotypes, hinting at a possible role of these cells in CMV control following haplo-HSCT with pt-cy. These data require additional, future investigations for confirmation.

References

1. Luznik L, O'Donnell P V, Symons HJ, et al. HLA-Haploidentical Bone Marrow Transplantation for Hematologic Malignancies Using Nonmyeloablative Conditioning and High-Dose, Posttransplantation Cyclophosphamide. Biol Blood Marrow Transplant. 2008;14(6):641-650.
2. Crocchiolo R, Bramanti S, Vai A, et al. Infections after T-replete haploidentical transplantation and high-dose cyclophosphamide as graft-versus-host disease prophylaxis. Transpl Infect Dis. 2015;17(2):242-249.
3. Levine JH, Simonds EF, Bendall SC, et al. Data-Driven Phenotypic Dissection of AML Reveals Progenitor-like Cells that Correlate with Prognosis. Cell. 2015;162(1):184-197.
4. Anderson BE, McNiff J, Yan J, et al. Memory CD4+ T cells do not induce graft-versus-host disease. J Clin Invest. 2003;112(1):101-108.
5. Chen BJ, Deoliveira D, Cui X, et al. Inability of memory T cells to induce graft-versus-host disease is a result of an abortive alloresponse. Blood. 2007;109(7):3115-3123.
6. Roberto A, Castagna L, Zanon V, et al. Role of naive-derived T memory stem cells in T-cell reconstitution following allogeneic transplantation. Blood. 2015;125(18):2855-2864.
7. Cieri N, Oliveira G, Greco R, et al. Generation of human memory stem T cells after haploidentical T-replete hematopoietic stem cell transplantation. Blood. 2015;125(18):2865-2874.
8. Kanakry CG, Ganguly S, Zahurak M, et al. Aldehyde dehydrogenase expression drives human regulatory T cell resistance to posttransplantation cyclophosphamide. Sci Transl Med. 2013;5(211):211ra157.
9. Wachsmuth LP, Patterson MT, Eckhaus MA, Venzon DJ, Gress RE, Kanakry CG. Posttransplantation cyclophosphamide prevents graft-versus-host disease by inducing alloreactive T cell dysfunction and suppression. J Clin Invest. 2019;129(6):2357-2373.
10. Suessmuth Y, Mukherjee R, Watkins B, et al. CMV reactivation drives posttransplant T-cell reconstitution and results in defects in the underlying TCRβ repertoire. Blood. 2015;125(25):3835-3850.
11. Kanakry CG, Coffey DG, Towlerton AMH, et al. Origin and evolution of the T cell repertoire after posttransplantation cyclophosphamide. JCI Insight. 2016;1(5):e86252.
12. Wills MR, Carmichael AJ, Mynard K, et al. The human cytotoxic T-lymphocyte (CTL) response to cytomegalovirus is dominated by structural protein pp65: frequency, specificity, and T-cell receptor usage of pp65-specific CTL. J Virol. 1996;70(11):7569-7579.
13. Huntley D, Giménez E, Pascual MJ, et al. Reconstitution of cytomegalovirus-specific T-cell immunity following unmanipulated haploidentical allogeneic hematopoietic stem cell transplantation with posttransplant cyclophosphamide. Bone Marrow Transplant. 2020;55(7):1347-1356.
14. Camargo JF, Wieder ED, Kimble E, et al. Deep functional immunophenotyping predicts risk of cytomegalovirus reactivation after hematopoietic cell transplantation. Blood. 2019;133(8):867-877.
15. Pelák O, Stuchlý J, Król L, et al. Appearance of cytomegalovirus-specific T-cells predicts fast resolution of viremia post hematopoietic stem cell transplantation.

Cytometry B Clin Cytom. 2017;92(5):380-388.

Figure legends

Figure 1. CMV reactivation impacts T-cell reconstitution following haplo-HSCT with pt-cy. **A**) Integrated median fluorescence intensity (iMFI) values, considering both expression level and frequency of marker$^+$ cells, of the CD8$^+$ or CD4$^+$ T-cell PhenoGraph clusters were visualized by heatmaps, while PhenoGraph cluster dynamics (median percentages of total CD8$^+$ or CD4$^+$ T-cells) in haplo-HSCT patients were revealed by balloon plots. **B**) PCA of CD8$^+$ and CD4$^+$ T-cell cluster frequencies. The left panel depicts the clusters driving the PCA, the central and right panel show the median PCA coordinates of all patients, grouped together or according to CMV viremia (subclinical viremia, *n*=6; clinical viremia, *n*=13; no viremia, *n*=2), per time point in months after transplant. The central and right panel should be read in conjunction with the left panel; the relative position of data points in the central and right panel is indicative of dominance of T-cell clusters shown with a similar relative position in the left panel. **C**) Dynamics of CD8$^+$ T_{EMRA}, CD4$^+$ T_{TE} T_H1 and CD8$^+$ naïve clusters in haplo-HSCT patients experiencing post-transplant CMV viremia. Medians with the number of patients per time point are shown and error bars represent interquartile range. Significance was determined by Kruskal-Wallis test and *P* values are shown at the upper border of the plot for each time point ($^*P < 0.05$). **D**) Flow cytometric analysis of CD45RA and T-bet expression in CD8$^+$ and CD4$^+$ T-cells at month 3 and month 6-8 after transplantation. For both CMV groups a single representative patient is shown. **E**) Hierarchical metaclustering using the Ward minimum variance method, of haplo-HSCT patients per month, based on the frequency of CD8$^+$ and CD4$^+$ T-cell PhenoGraph clusters. aGVHD, acute graft-versus-host disease; Exh, exhausted; PB, peripheral blood; Prolif, proliferating; T_{CM}, central memory; T_{EF}, effector; T_{EM}, effector memory; T_{EMRA}, effector memory re-expressing CD45RA; T_M, memory; T_{REG}, regulatory T-cell; T_{TE}, terminal effector; T_{TM}, transitional memory.

Figure 2. High-dimensional single-cell profiling reveals the dynamics of the CMV-specific T-cell response following haplo-HSCT with pt-cy. A) UMAP analysis of cytokine-positive $CD8^+$ and $CD4^+$ T-cells from PBMC samples stimulated overnight with CMV pp65 peptide mix. Graphs highlight events belonging to different time points or events positive for a given marker. **B**) Heatmaps depict marker expression in normalized iMFI values of the antigen-specific $CD8^+$ or $CD4^+$ T-cell PhenoGraph clusters. Balloon plots show the median cluster frequencies as percentage of total $CD8^+$ or $CD4^+$ T-cells in haplo-HSCT patients experiencing post-transplant CMV viremia, after background correction was applied. **C**) Polyfunctionality of the CMV-specific T-cell response over time in months post-transplant, as determined by assessment of expression of cytokines IFN-γ, TNF and IL-2, and degranulation marker CD107a by cell clusters identified in (B). Measurements containing < 50 CMV-specific cells after background correction were discarded from analysis. Medians are depicted and error bars represent the interquartile range. Significance was determined by Kruskal-Wallis test with post-hoc Dunn's test ($^{*}P < 0.05$, $^{**}P < 0.01$; $^{***}P < 0.001$). **D**) Balloon plots show the median cluster frequencies as percentage of CMV-specific $CD8^+$ or $CD4^+$ T-cells at month 10-13 compared to that found in the graft, PB of the donor and PB of unrelated healthy controls, after background correction was applied. Measurements containing < 50 CMV-specific cells after background correction were discarded from analysis. Exh, exhausted; HC, healthy control; Mult, multifunctional; PB, peripheral blood; Prolif, proliferating; T_{CM}, central memory; T_{EF}, effector; T_{EM}, effector memory; T_{EMRA}, effector memory re-expressing CD45RA; T_{TE}, terminal effector.

Figure 3. CMV viremia control following haplo-HSCT with pt-cy associates with the development of distinct CD4$^+$ antigen-specific T-cell immunophenotypes. A) Total CMV-specific CD8$^+$ or CD4$^+$ T-cell counts and **B**) cluster-specific T-cell counts in the blood of haplo-HSCT patients with subclinical (*n*=6) or clinical (*n*=13) CMV viremia during the first year post-transplant. Medians with the number of patients per time point are shown and error bars represent interquartile range. Significance was determined by Kruskal-Wallis test and *P* values are shown at the upper border of the plot for each time point ($^*P < 0.05$). Mult, multifunctional; Prolif, proliferating; T_{TE}, terminal effector.

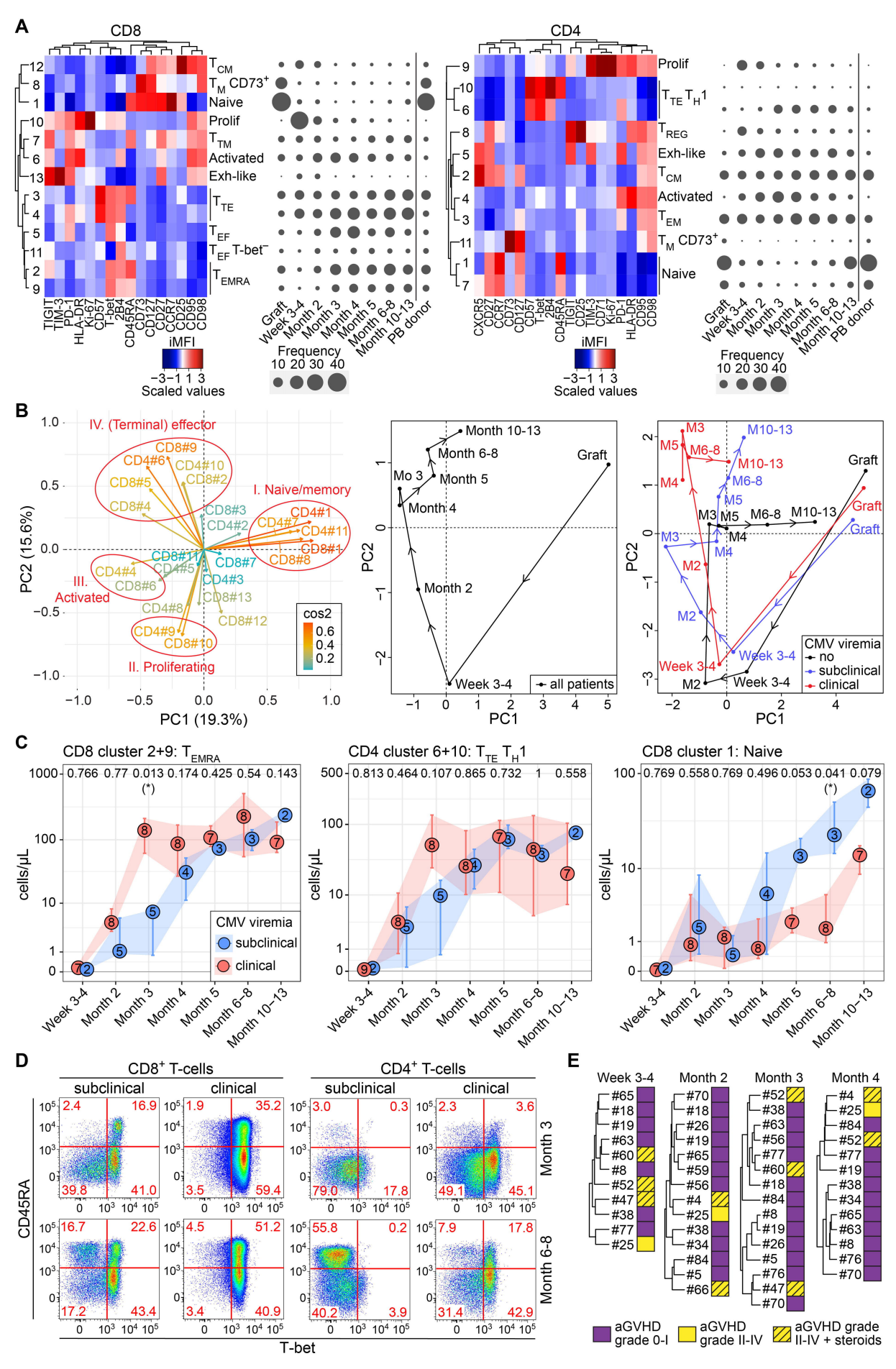
A
CD8
CD4
T_CM
T_M CD73+
Naive
Prolif
T_TM
Activated
Exh-like
T_TE
T_EF
T_EF T-bet−
T_EMRA
T_TE T_H1
T_REG
T_EM
iMFI
Scaled values
Frequency
Graft
Week 3-4
Month 2
Month 3
Month 4
Month 5
Month 6-8
Month 10-13
PB donor
B
IV. (Terminal) effector
I. Naive/memory
III. Activated
II. Proliferating
cos2
PC1 (19.3%)
PC2 (15.6%)
all patients
CMV viremia
no
subclinical
clinical
C
CD8 cluster 2+9: T_EMRA
CD4 cluster 6+10: T_TE T_H1
CD8 cluster 1: Naive
cells/µL
D
CD8+ T-cells
CD4+ T-cells
subclinical
clinical
CD45RA
T-bet
Month 3
Month 6-8
E
aGVHD grade 0-I
aGVHD grade II-IV
aGVHD grade II-IV + steroids

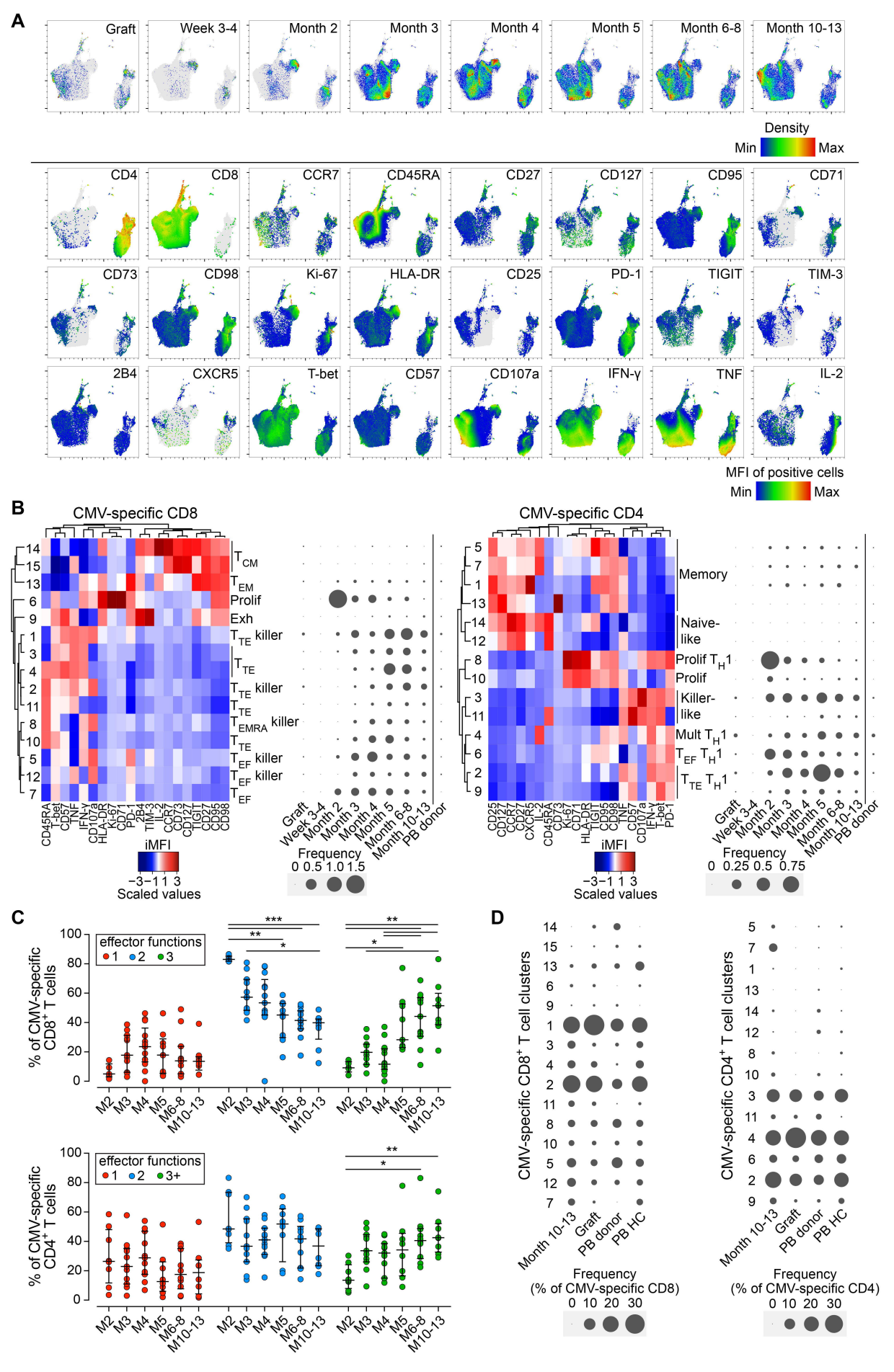
A
Graft
Week 3-4
Month 2
Month 3
Month 4
Month 5
Month 6-8
Month 10-13
Density
Min
Max
CD4
CD8
CCR7
CD45RA
CD27
CD127
CD95
CD71
CD73
CD98
Ki-67
HLA-DR
CD25
PD-1
TIGIT
TIM-3
2B4
CXCR5
T-bet
CD57
CD107a
IFN-γ
TNF
IL-2
MFI of positive cells
Min
Max
B
CMV-specific CD8
CMV-specific CD4
T_CM
T_EM
Prolif
Exh
T_TE killer
T_TE
T_TE killer
T_TE
T_EMRA killer
T_TE
T_EF killer
T_EF killer
T_EF
Memory
Naive-like
Prolif T_H1
Prolif
Killer-like
Mult T_H1
T_EF T_H1
T_TE T_H1
CD45RA T-bet CD57 TNF IFN-γ CD107a HLA-DR Ki-67 PD-1 2B4 TIM-3 IL-2 CCR7 CD73 CD127 TIGIT CD27 CD95 CD98
CD25 CD127 CCR7 CD27 CXCR5 IL-2 CD45RA CD73 Ki-67 CD71 HLA-DR CD95 CD98 TNF CD57 CD107a IFN-γ T-bet PD-1
iMFI
−3 −1 1 3
Scaled values
Graft
Week 3-4
Month 2
Month 3
Month 4
Month 5
Month 6-8
Month 10-13
PB donor
Frequency
0 0.5 1.0 1.5
Frequency
0 0.25 0.5 0.75
C
% of CMV-specific CD8+ T cells
% of CMV-specific CD4+ T cells
effector functions
1 2 3
1 2 3+
M2 M3 M4 M5 M6-8 M10-13
D
CMV-specific CD8+ T cell clusters
CMV-specific CD4+ T cell clusters
Month 10-13
Graft
PB donor
PB HC
Frequency
(% of CMV-specific CD8)
0 10 20 30
Frequency
(% of CMV-specific CD4)
0 10 20 30

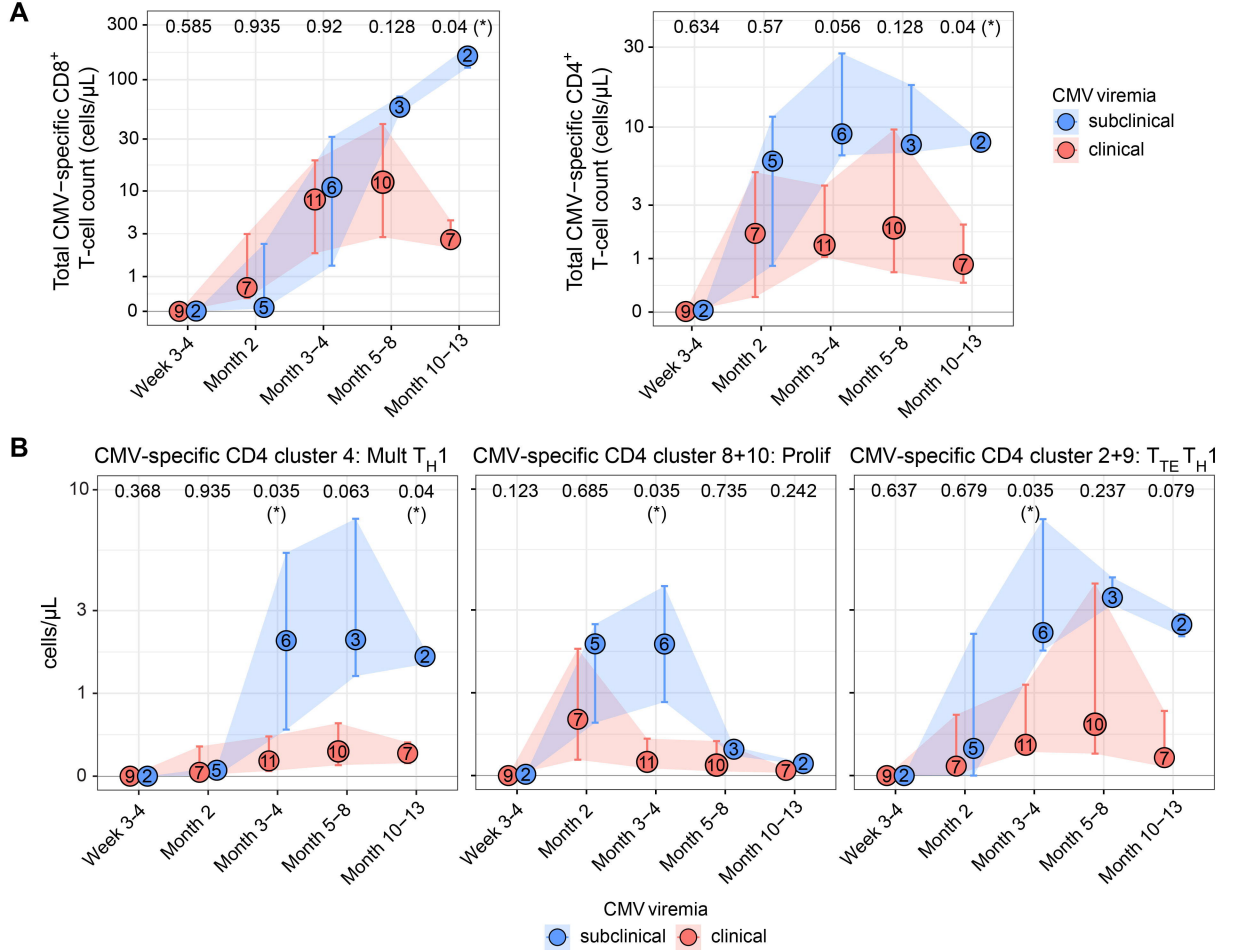
A
Total CMV−specific CD8+ T-cell count (cells/µL)
0.585 0.935 0.92 0.128 0.04 (*)
Total CMV−specific CD4+ T-cell count (cells/µL)
0.634 0.57 0.056 0.128 0.04 (*)
Week 3–4
Month 2
Month 3–4
Month 5–8
Month 10–13
CMV viremia
subclinical
clinical
B
CMV-specific CD4 cluster 4: Mult TH1
0.368 0.935 0.035 0.063 0.04
CMV-specific CD4 cluster 8+10: Prolif
0.123 0.685 0.035 0.735 0.242
CMV-specific CD4 cluster 2+9: TTE TH1
0.637 0.679 0.035 0.237 0.079
cells/µL
CMV viremia
subclinical
clinical

Table S1. Patient characteristics and treatment.

ID	D/R Sex	D/R Age	Pathology	Conditioning	Graft type	GVHD prophylaxis[f]	aGVDH grade	Steroid therapy	CMV D/R	CMV viremia	CMV viremia onset	Antiviral treatment	Blood samples analyzed
#4	M/F	52/22	HL	Baltimore[a]	BM	FK	2	Yes	-/+	subclinical	day 57	Ganciclovir	day 56, 99, 126, 180, 386
#5	F/M	64/53	NHL	Baltimore[a]	BM	FK	No	No	+/+	subclinical	day 30	No	day 44, 57, 63
#8	F/F	61/33	HL	Baltimore[a]	BM	FK	No	No	+/+	subclinical	day 49	No	day 28, 74, 88, 112
#18	M/M	51/25	NHL	Baltimore[a]	BM	FK	1	No	+/+	No	NA	No	day 21, 29, 36, 43, 68, 75, 127, 369
#19	F/M	38/57	HL	Baltimore[a]	BM	FK	1	No	+/+	subclinical	day 33	No	day 29, 36, 43, 50, 68, 92, 113
#25	M/M	35/62	NHL	Baltimore[a]	BM	FK	2	No	+/-	clinical	day 55	Ganciclovir	graft and day 28, 42, 49, 58, 97, 121, 216, 349
#26	F/F	49/42	NHL	Baltimore[a]	BM	FK	1	No	+/+	subclinical	day 48	No	day 44, 51, 69, 76, 153, 202, 331
#34	F/M	63/33	AML	TBF MAC[b]	BM	FK	No	No	+/+	clinical	day 40	Ganciclovir	day 21, 29, 40, 96, 124, 190, 363
#38	F/M	27/35	ALL	TBF MAC[b]	BM	CsA	No	No	+/+	clinical	day 32	Ganciclovir	graft and day 28, 42, 74, 102, 144
#47	M/F	45/47	NHL	Baltimore[a]	BM	CsA	2	Yes	+/+	clinical	day 50	Ganciclovir	graft and day 28, 76
#52	M/M	53/38	HL	RIC[c]	BM	CsA	2	Yes	+/-	clinical	day 32	Valganciclovir	graft and day 22, 28, 67, 112, 182, 330
#56	F/F	29/28	HL	GITMO[d]	BM	CsA	No	No	+/+	clinical	day 14	Valganciclovir	graft and day 49, 83
#59	M/M	32/70	MDS	TBF RIC[e]	PBSC	CsA	No	No	+/+	clinical	day 32	Ganciclovir - Valganciclovir	graft and day 21, 36
#60	M/M	47/20	HL	Baltimore[a]	PBSC	CsA	2	Yes	-/+	clinical	day 39	Ganciclovir - Foscarnet	graft and day 21, 26, 64, 82, 141, 169, 348
#63	M/M	28/25	HL	Baltimore[a]	PBSC	CsA	No	No	+/-	clinical	day 41	Ganciclovir - Valganciclovir	graft and day 21, 27, 62, 100, 136, 161, 204, 282
#65	M/M	37/69	MDS	TBF RIC[e]	BM	CsA	1	No	-/+	clinical	day 31	Ganciclovir - Valganciclovir	day 21, 42, 59, 101, 126, 191, 302
#66	F/M	30/68	AML	TBF RIC[e]	PBSC	CsA	4	Yes	+/+	clinical	day 27	Ganciclovir	graft and day 38, 139
#70	F/M	40/36	ALL	TBF MAC[b]	PBSC	CsA	1	No	+/-	clinical	day 48	Valganciclovir	graft and day 48, 76, 104, 142, 167, 371
#76	M/F	33/56	HL	RIC[c]	BM	CsA	1	No	+/+	clinical	day 27	No	graft and day 90, 111, 223
#77	M/F	61/26	HL	Baltimore[a]	BM	CsA	1	No	+/-	No	NA	No	graft and day 27, 79, 121, 177, 205, 359
#84	M/M	25/52	MF	Baltimore[a]	PBSC	CsA	No	No	-/+	subclinical	day 95	No	graft and day 48, 62, 100, 146, 184, 219

[a]See Luznik et al.[1]

[b]TBF MAC: thiotepa 10 mg/kg, busulfan 3.6 mg/kg, fludarabine 150 mg/m^2

[c]RIC: thiotepa 10 mg/kg, cyclophosphamide 30 mg/kg, fludarabine 60 mg/m^2

[d]GITMO: thiotepa 10 mg/kg, cyclophosphamide 60 mg/kg, fludarabine 60 mg/m^2

[e]TBF RIC: thiotepa 5 mg/kg, busulfan 6.4 mg/kg, fludarabine 150 mg/m^2

[f]All patients received pt-cy and mycophenolate mofetil

ALL, acute lymphoid leukemia; AML, acute myeloid leukemia; BM, bone-marrow; CsA, cyclosporine A; D, donor; F, female; FK, tacrolimus; HL, Hodgkin lymphoma; M, male; MAC, myeloablative conditioning; MDS, myeloid dysplastic syndrome; MF, myelofibrosis; NA, not applicable; NHL, non-Hodgkin lymphoma; PBSC, peripheral blood stem cells; R, recipient; RIC, reduced intensity conditioning; TBF, thiotepa-busulfan-fludarabine

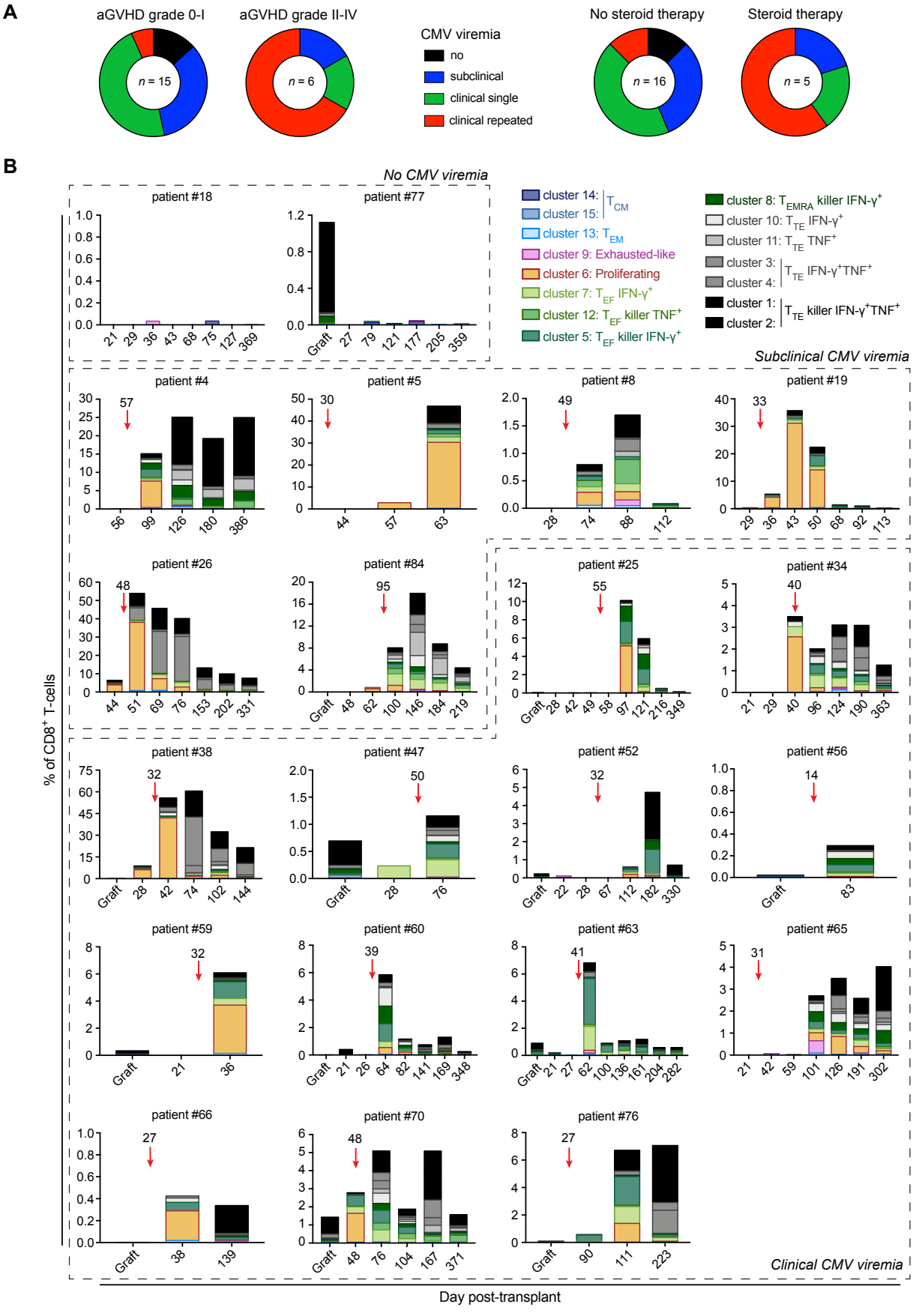

Figure S1. Impact of aGVHD and corticosteroid therapy on CMV reactivation, and longitudinal high-dimensional profiling of CMV-specific CD8$^+$ T-cells in recipients of haplo-HSCT with pt-cy. A) CMV reactivation among recipients of haplo-HSCT with pt-cy, stratified by occurence of aGVDH or corticosteroid therapy. **B**) Frequencies of CMV-specific CD8$^+$ T-cell PhenoGraph clusters among total CD8$^+$ T-cells are shown for all measured time points. Arrows indicate the day post-transplant of CMV viremia onset. Patients are grouped according to post-transplant CMV viral load.

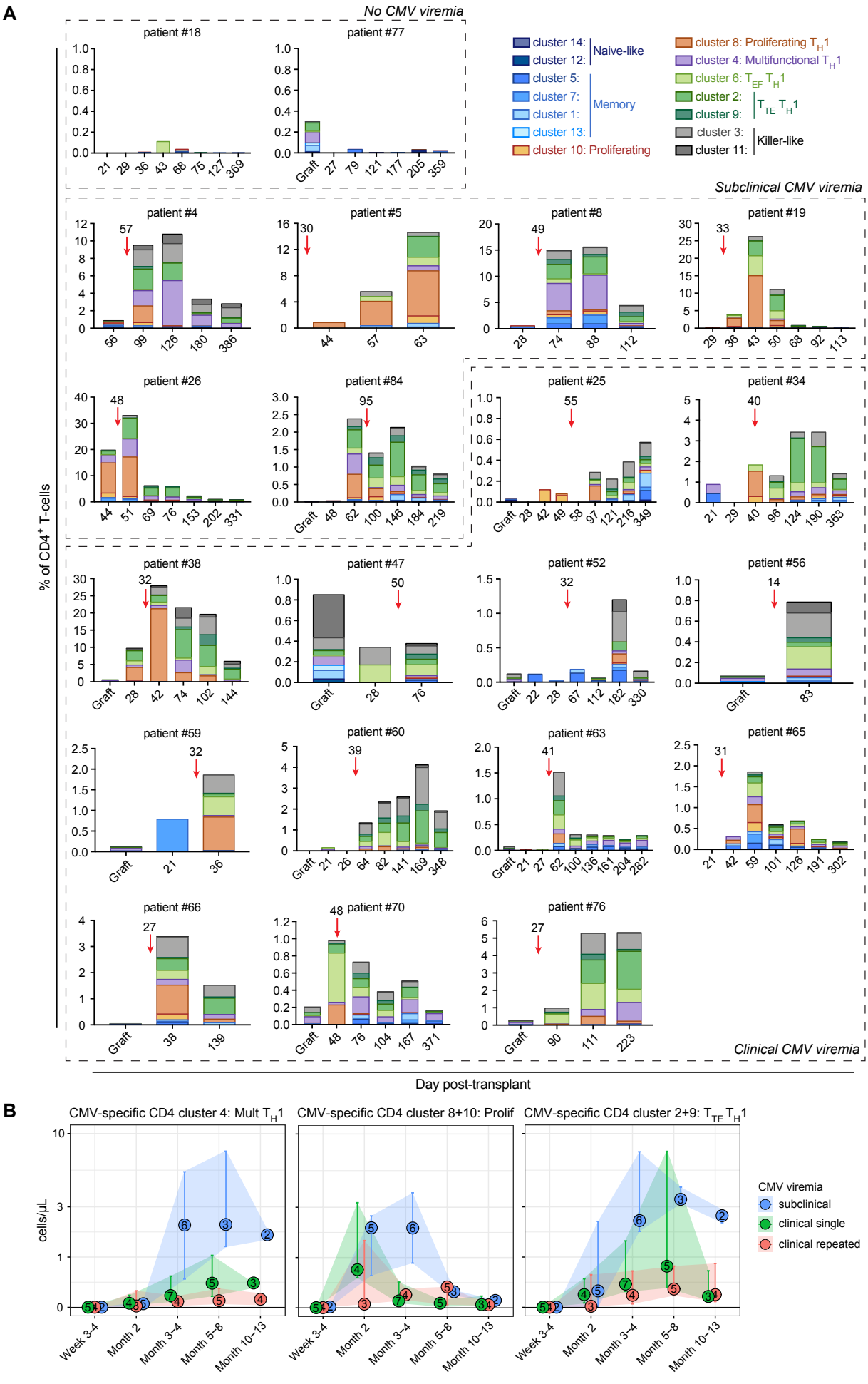

Figure S2. CMV viremia control following haplo-HSCT with pt-cy associates with the development of distinct CD4⁺ antigen-specific T-cell immunophenotypes. A) Frequencies of CMV-specific CD4⁺ T-cell PhenoGraph clusters among total CD4⁺ T-cells are shown for all measured time points. Arrows indicate the day post-transplant of CMV viremia onset. Patients are grouped according to post-transplant CMV viral load. **B**) CMV-specific CD4⁺ T-cell counts in the blood of haplo-HSCT patients experiencing CMV viremia during the first year post-transplant. Medians with the number of patients per time point are shown and error bars represent interquartile range.